

Production and detection of high-energy neutrinos from Cygnus X-3

Edward W. Kolb, Michael S. Turner, and Terry P. Walker

NASA/Fermilab Astrophysics Center, Fermi National Accelerator Laboratory, P.O. Box 500, Batavia, Illinois 60810

(Received 12 March 1985; revised manuscript received 3 June 1985)

Cygnus X-3 is a potent source of high-energy γ rays, with energies up to 10^4 TeV. In the context of a model where these γ rays are produced by the collision of a high-energy proton beam with matter we calculate the flux, spectrum, and "light curve" of the neutrinos produced. Neutrinos with energies of 3–100 TeV may be detectable in large, underground detectors by the muons they produce in the surrounding rock.

I. THE CYGNUS X-3 SYSTEM

The Cygnus X-3 system is a very robust source of radio, infrared (IR), x-ray, medium-energy (ME) γ ray (~ 100 MeV), and ultra high-energy (UHE) γ ray (> 100 TeV) photons. A 4.8-h period is observed in all but the radio emission and appears to be associated with the orbital period of a binary system, thought to consist of a compact object (possibly a young pulsar) and $\sim 4M_{\odot}$ companion.^{1,2} Eclipsing of the compact object by the companion is believed to be responsible for the observed periodicity (see Fig. 1).

Characteristics of the light curves from Cygnus X-3 allow one to construct models of the system. The x-ray light curve does not contain a zero-flux minimum but instead is smoothed to a sinusoid.¹ The absence of a complete x-ray eclipse can be understood if the binary system is shrouded by a cocoon of optical depth unity for x rays, which scatters x rays originating from the compact object during eclipse.^{3,4} ME γ rays from the compact object pass directly through the cocoon without being scattered, resulting in the zero-flux minimum (centered about x ray minimum which we take to occur at phase $\psi=0$) observed by Lamb *et al.*⁵ at ~ 100 MeV. The duration of the eclipse ($\Delta\psi \approx 40\%$) and the orbital period establishes an upper limit for the companion mass of $4M_{\odot}$, assuming a $1.4M_{\odot}$ compact object.

Although the UHE γ -ray light curve exhibits a 4.8-h period, it is much different in structure than those observed in IR, x ray, and ME γ ray, suggesting a different mechanism for the UHE photon production. The UHE γ -ray light curve seems to show two pulses, occurring just before and just after x-ray minimum separated by 0.4 in phase, and having a width $\Delta\psi \leq 0.05$. The mean UHE γ -ray flux above 2 TeV in the pulses is^{6–8} $\sim 10^{37}$ erg/sec. In addition, a 4.8-h periodic signal from Cygnus X-3 has been detected in the energy range 2×10^{15} eV to 2×10^{16} eV by Samorski and Stamm⁹ and Lloyd-Evans *et al.*⁹ Their data, combined with lower-energy measurements, can be fit by a power-law spectrum:

$$dN_{\gamma}/dE \approx 3 \times 10^{-10} E^{-2.1} \text{ cm}^{-2} \text{ sec}^{-1} \quad (1.1)$$

(E in TeV) for the *average* photon flux. The uncertainty

in the slope is 2% and in the normalization a factor of 2. Assuming isotropic emission and a distance of¹⁰ 12 kpc, the luminosity of Cygnus X-3 above 1 GeV is $\sim 10^{38}$ erg sec⁻¹, making it the brightest γ -ray point source in the galaxy.

Vestrand and Eichler² have proposed the following model for the UHE- γ -ray flux from Cygnus X-3. The compact object is a source of UHE protons which collide with the companion star, producing π^0 's whose subsequent decays lead to UHE photons. If the region of neutral- π production is optically thin to TeV photons, they can pass through the companion and are observed. Only for a small fraction of the orbital phase, around the time that line of sight to the compact object just grazes the companion star¹¹ ($\psi \approx \pm 0.25$), are both of these conditions met—sufficient material to produce π^0 's and optical depth from the production site to the observer of less than order unity, thereby accounting for the two narrow UHE- γ -ray pulses which are observed.

In addition to making π^0 's, pN interactions in the companion will also produce π^{\pm} 's whose decays results in a ν_{μ} flux from the system.^{2,12} In this paper we will discuss the characteristics of the neutrino flux from Cygnus X-3 and the possibility of detecting these neutrinos in large, underground detectors.¹³

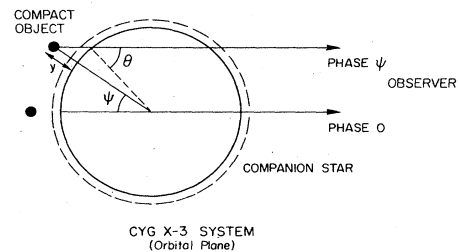


FIG. 1. A schematic diagram of the Cygnus X-3 system. The dashed circle shows the atmosphere, y is the distance between the compact object and the surface of the companion star, ψ is the phase angle, and θ is the angle between the line of sight and the line which connects the intersection of the line of sight with the star and the center of the star. We have omitted the shroud from this diagram and have assumed that the line of sight lies in the orbital plane.

II. HIGH-ENERGY NEUTRINO PRODUCTION IN CYGNUS X-3

In this section we use the UHE photon spectrum to calculate the spectrum and phase diagram of the neutrinos that also must be produced. The origin and spectrum of the incident proton beam is irrelevant for our purposes. We need only assume that π^0 , π^+ , and π^- are produced in equal numbers.

If the UHE γ rays originate from a source spectrum of the form

$$\frac{dS_\gamma(E_\gamma)}{dE_\gamma} = AE^{-n}, \quad (2.1)$$

and are produced by π^0 decays, then the π^0 source spectrum is inferred to be

$$\frac{dS_{\pi^0}(E_\pi)}{dE_\pi} = A2^{n-1}E^{-n}, \quad (2.2)$$

where the factors of 2 come from counting two photons of energy $E_\pi/2$ from each π^0 decay. There should also be π^+ 's and π^- 's produced in numbers comparable to π^0 , and

$$dS(\pi^+ + \pi^-)/dE = 2 dS_{\pi^0}/dE.$$

The π^\pm decays will produce neutrinos with an energy that depends upon whether the π^\pm 's decay in flight, or interact before decay. For the moment we will assume the π^\pm 's decay in flight, and later we will discuss the conditions under which the π^\pm 's interact before decay. K mesons will also be produced by the proton interactions, however, at only about 10% of the rate at which π^\pm 's are produced. Their decays will also produce ν_μ 's.

The decay of a π^\pm in flight produces a neutrino of energy

$$E_\nu = E_\pi(1 - m_\mu^2/m_\pi^2)/2,$$

which leads to a neutrino-source spectrum of¹⁴

$$\frac{dS_\nu(E_\nu)}{dE_\nu} = (1 - m_\mu^2/m_\pi^2)^n \frac{dS_\gamma(E_\gamma)}{dE_\gamma}. \quad (2.3)$$

In order to relate the source spectrum to the observed number spectrum it is necessary to propagate the source spectrum through the companion star. The absorption of the γ 's and ν 's by the star depends upon the column density material encountered by the γ or ν traversing the star, which in turn depends upon the phase ψ .¹¹

The photons can only traverse the star when the source is near phase $\psi \simeq \pm 0.25$. Since the γN cross section at high energies is roughly energy independent, the relative intensity of the UHE photon flux should be energy independent, and appear only at phase $\psi \simeq \pm 0.25$. The UHE photons are detected for a total phase of $(\Delta\psi)_\gamma \approx 0.05$. Although a normal stellar model would result in $(\Delta\psi)_\gamma$ at least a factor of 10 smaller, the companion star in this system is expected to be significantly altered by the compact object,² which can easily account for the large $(\Delta\psi)_\gamma$.

Due to their weak-interaction cross section neutrinos more easily traverse the star. However, very energetic neu-

trinos are not able to traverse the star around phase $\psi=0$, and the phase diagram for UHE neutrinos will also show an eclipse. Unlike the photons, the neutrino cross section is energy dependent, and the phase diagram (or "light curve") for neutrinos will reflect this energy dependence.

The incident neutrino beam is reduced while traversing the star by a factor of $\exp[-\int \sigma n(x)dx]$, where σ is the total cross section for muon production, $\nu_\mu N \rightarrow \mu X$, and n is the number density of nucleons. At energies below about 100 TeV, the cross section increases linearly with energy, and above 100 TeV the cross section increases only logarithmically, due to the effect of the W -boson propagator,¹⁵

$$\sigma = 7 \times 10^{-36} E \text{ cm}^2, \quad E \leq 100 \text{ TeV}, \quad (2.4a)$$

$$\sigma = 1.2 \times 10^{-34} \ln E \text{ cm}^2, \quad E \geq 100 \text{ TeV} \quad (2.4b)$$

(E in TeV). At energies below 100 TeV the antineutrino cross section is one-half this value, while at energies above 100 TeV the two cross sections are roughly equal. We estimate $\int n(x)dx$ by assuming that the companion star has radius of $R = 2R_\odot$, a central density of 30 g cm^{-3} , and a density profile given by

$$\rho(r) = \rho_c \exp(-12r/R).$$

We find that neutrino absorption is more sensitive to the central density than to the parametrization of the density profile. Although a central density of 30 g cm^{-3} may be reasonable for a normal $4M_\odot$ main-sequence star,¹⁶ the structure of a $4M_\odot$ star with a companion compact object orbiting at a distance of order its radius may well be quite different. We have calculated neutrino absorption with different central densities (and the results are qualitatively similar). In principle the absorption also depends upon the mass of the companion; for normal main-sequence stars the density profiles are rather similar, i.e., a function of r/R and the central density only, and $R \propto M^{0.6}$. This implies that $\int n(x)dx \propto M^{0.2}$ is rather insensitive to the mass of the star.

The effect of absorption of neutrinos is shown in Fig. 2.

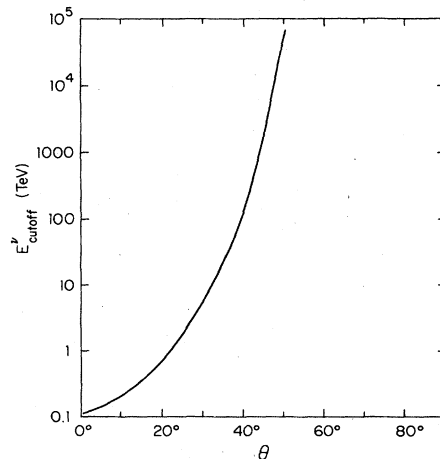


FIG. 2. The neutrino cutoff energy E_{cutoff}^ν , determined by $\int n(x)\sigma(E_{\text{cutoff}}^\nu)dx = 1$, as a function of θ (see Fig. 1), computed for a $4M_\odot$ star.

At energies above 100 TeV, the absorption cross section is relatively energy independent, so all energies above 100 TeV will have the same phase structure for the *relative* intensity. The predicted neutrino light curves are shown in Fig. 3.

We now return to the question of whether or not the K 's and π 's decay in flight. The decay distance (λ_D) of π^\pm 's and K^\pm 's in the star frame is

$$\begin{aligned} (\gamma c \tau)_{\pi^\pm} &= 5.3 \times 10^6 E \text{ cm}, \\ (\gamma c \tau)_{K^\pm} &= 7.5 \times 10^5 E \text{ cm} \end{aligned} \quad (2.5)$$

(E in TeV). The cross section for the (π, K) interaction is $\sigma_I \simeq 3 \times 10^{-26} \text{ cm}^2$ at high energies (\gtrsim TeV) and so the interaction distance is

$$\lambda_I = (n \sigma_I)^{-1} = (6 \times 10^7 / \rho_{-6}) \text{ cm}, \quad (2.6)$$

where $\rho_{-6} = (\rho / 10^{-6}) \text{ cm}^{-3}$. Since the decay length is less than the scale height for density change in the star we have assumed a constant density in Eq. (2.6).¹⁷

There will be a cutoff energy, above which mesons will interact before decaying. We estimate this energy by setting $3\lambda_I = \lambda_D$. This critical energy is given by

$$E_c \simeq \begin{cases} (300 / \rho_{-6}) \text{ TeV} & (K^\pm), \\ (30 / \rho_{-6}) \text{ TeV} & (\pi^\pm). \end{cases} \quad (2.7)$$

Therefore the source function for neutrinos produced by K 's and π 's should be cut off at an energy of the order of $E_c \simeq (100 / \rho_{-6}) \text{ TeV}$. (More precisely, the slope of dN_ν/dE will steepen by one unit, $E^{-n} \rightarrow E^{-n-1}$, as a fraction ($\propto E^{-1}$) of the π^\pm 's that will decay before interacting.) The cutoff energy is most sensitive to the density in the envelope of the star. By detection of E_c it is possible to gain information about the density in the envelope. In addition to π 's and K 's, charm and other heavy flavors will be produced. The lifetimes of D and F charmed mesons are less than 10^{-12} sec, and they will decay promptly and produce neutrinos before interacting. At energies greater than E_c the neutrino flux will be due to prompt decays (as in a beam-dump-type experiment).

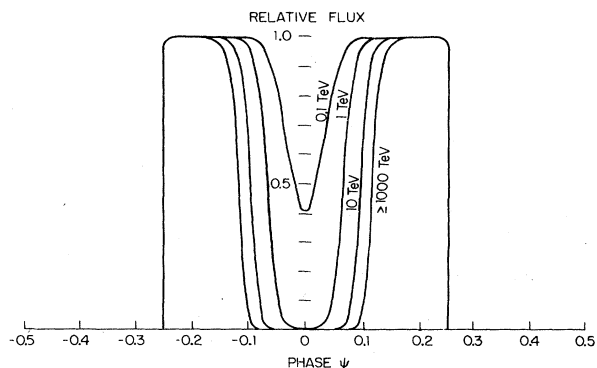


FIG. 3. The neutrino light curve for different neutrino energies. In constructing the light curve we have assumed that $i \simeq 90^\circ$ and $y/R < 1$ so that $\theta \simeq \psi$ (see Fig. 1 and Ref. 11). Since the muon events in an underground detector are primarily due to neutrinos of energy of order 10 TeV, that is the light curve which would be observed.

However the efficiency for charm and heavy-flavor production is expected to be 10^{-2} – 10^{-3} that of π, K production. Therefore above E_c the flux the neutrinos will be suppressed by 10^2 – 10^3 .

Some fraction of the π 's and K 's initially more energetic than E_c will interact and have their energy degraded to less than E_c before they decay or are absorbed. Once the energy of a π or K has been reduced to the order of E_c it will on average decay before interacting again. Thus we expect some "piling up" of those π 's and K 's initially more energetic than E_c at an energy $\simeq E_c$, in turn leading to more decay neutrinos of energy E_c . If the initial spectrum of π 's and K 's decreases with energy this will be a small effect (at most order unity). However, if the initial spectrum of π 's and K 's is approximately monoenergetic this could be a very important effect—as we will discuss in the next section.

We can now relate dN_ν/dE to dN_γ/dE . Using the observed photon spectrum from Eq. (1.1), we infer the phase-averaged neutrino spectrum (for $E < E_c$)

$$\frac{dN_\nu}{dE} \simeq (1 - m_\mu^2/m_\pi^2)^{2.1} \frac{(\Delta\psi)_\nu}{(\Delta\psi)_\gamma} \frac{dN_\gamma}{dE}. \quad (2.8)$$

Although $(\Delta\psi)_\nu$ is energy dependent, $(\Delta\psi)_\nu \simeq 0.4$ is a good approximation for all energies. Therefore

$$dN_\nu/dE \simeq 4 \times 10^{-10} E^{-2.1} \text{ cm}^{-2} \text{ sec}^{-1} \quad (E < E_c) \quad (2.9)$$

(E in TeV) and about 10^2 – 10^3 times smaller for $E > E_c$. We note that the normalization of the predicted neutrino spectrum is uncertain by at least a factor of order 10, due to uncertainties in $\Delta\psi_\gamma$, the photon spectrum, and the possibility of some absorption of UHE photons even during the bright phase. (In fact it is very likely that there is some photon absorption, since a column density of order 60 g cm^{-2} is needed to produce pions, while a column density of order 20 g cm^{-2} is needed for UHE photons to be absorbed.) In the next section we use this result to calculate count rates in large, underground detectors.

III. PROSPECTS FOR DETECTION IN LARGE, UNDERGROUND DETECTORS

Consider a large (of the order of 1000 m^3), underground (distance d below the surface) detector, shown schematically in Fig. 4. For example, the Irvine-Michigan-Brookhaven (IMB) proton-decay detector¹⁸ is $23 \text{ m} \times 18 \text{ m} \times 17 \text{ m}$ and 1500 m of water equivalent (mwe) below ground. Such a detector can detect neutrinos which (1) interact within the detector or (2) produce muons in the surrounding rock which have sufficient energy to get to and pass through the detector. We will call the first type of event a "contained" event and the second type of event a "muon" event.

The probability that a neutrino which is passing through the detector interacts in the detector is

$$\begin{aligned} P_c(E) &\simeq n \sigma l \\ &\simeq \begin{cases} 4 \times 10^{-9} I_{10} E & (E \lesssim 100 \text{ TeV}), \\ 7 \times 10^{-8} I_{10} \ln E & (E \gtrsim 100 \text{ TeV}), \end{cases} \end{aligned} \quad (3.1)$$

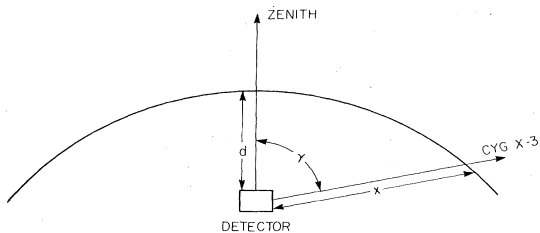


FIG. 4. Schematic diagram of the detector. The distance below the surface is d , the zenith angle of Cygnus X-3 is γ , and the distance to the surface at zenith angle γ is x .

where $l = l_{10} \times (10 \text{ m})$ is the typical (water equivalent) linear dimension of the detector,¹⁹ E is in TeV, σ is the cross section for $\nu_{\mu} + N \rightarrow \mu^{-} + X$ [see Eq. (2.4)], and $n = 6 \times 10^{23} \text{ cm}^{-3}$ is the number density of target nuclei.

Relativistic muons lose energy at the rate (per cm water equivalent)²⁰

$$-dE/dx \simeq 1.9 \times 10^{-6} \text{ TeV cm}^{-1} + (4 \times 10^{-6} \text{ cm}^{-1}) E. \quad (3.2)$$

Integrating this we find that the range of a relativistic muon is

$$L(E) \simeq (3 \times 10^5 \text{ cm}) \ln[1 + 2E_{\mu}/(1 \text{ TeV})] \simeq (5 \times 10^5 \text{ cm}) E_{\mu}/(1 \text{ TeV}) \quad (E_{\mu} \leq 1 \text{ TeV}) \quad (3.3)$$

which rises linearly with energy up to an energy of about a TeV and only logarithmically thereafter. Muons produced within a distance $L(E_{\mu})$ of the detector will have sufficient energy to make it to the detector. Thus the effective linear size of the detector for muon-type events is $L(E_{\mu})$. Of course, this size can be no larger than the distance from the detector to the earth's surface x (see Fig. 4). The probability that a neutrino of energy E (in TeV) interacts in the rock outside the detector and produces a muon which passes through the detector is

$$P_{\mu}(E) = \int_0^E \sigma(E_{\mu}) L(E_{\mu}) f(E_{\mu}) dE_{\mu} \simeq 1.0 \times 10^{-6} E [\ln(1 + E)], \quad (3.4)$$

(E in TeV) where $f(E_{\mu}) dE_{\mu}$ is the probability that the muon produced has an energy between E_{μ} and $E_{\mu} + dE_{\mu}$. For simplicity we have assumed that the typical muon energy is about equal to half that of the incident neutrino.²¹ Notice that the ratio P_{μ}/P_c increases with energy, and for neutrinos more energetic than a few l_{10} GeV the effective size of the detector for muon events is larger than that for contained events. Thus if the neutrinos are predominantly very high energy ($> \text{TeV}$) the contained type events should be rare.

The event rate in the detector is given in terms of the neutrino spectrum dN_{ν}/dE and the probability $P(E)$ that a neutrino of energy E interacts:

$$\Gamma_i \simeq a \int P_i(E) (dN_{\nu}/dE) dE, \quad (3.5)$$

where a is the cross-sectional area presented by the detector. We assume a differential spectrum of the form: $dN_{\nu}/dE = AE^{-n}$. For a spectral index $n < 3$ the muon events are dominated by the highest-energy events. The integral in Eq. (3.5) is cut off by the logarithmic dependence of $L(E)$ for $E > \text{few TeV}$, or the cutoff in the spectrum discussed in the preceding section, E_c , if E_c is less than a few TeV:

$$\Gamma_{\mu} = aA \times 1.0 \times 10^{-6} \int E^{-n+1} \ln(1+E) dE \simeq aA \times 1.0 \times 10^{-6} \int (u-1)^{-n+1} \ln u du, \quad (3.6)$$

where $u = 1 + E$. The dimensionless integral in Eq. (3.6) has the values 200, 20, 14, 5.0, 4.5 for $n = 1.5, 2, 2.1, 2.5, 2.75$. Half the contribution to the integral comes from neutrino events with energies between 3 and 100 TeV.

The contained events on the other hand dominated by the low-energy events (as long as $n > 2$):

$$\Gamma_c \simeq a l_{10} A \times 4 \times 10^{-9} \int E^{-n+1} dE \simeq a l_{10} A \times 4 \times 10^{-9} \times 10^{3(n-2)} \times (E_{\min}/1 \text{ GeV})^{-n+2}, \quad (3.7)$$

where E_{\min} is the larger of the detector threshold and the low-energy cutoff in the neutrino spectrum. The ratio of the two types of events is given by

$$\Gamma_{\mu}/\Gamma_c \simeq 250(1000)^{2-n} l_{10}^{-1} \times \left[\int (u-1)^{-n+1} \ln u du \right] \times (E_{\min}/1 \text{ GeV})^{n-2}. \quad (3.8)$$

For the neutrino spectrum derived from the high-energy photon spectrum ($A \simeq 4 \times 10^{-10} \text{ cm}^2 \text{ sec}^{-1}$ and $n = 2.1$) and a detector cross section of order $4 \times 10^6 \text{ cm}^2$ the predicted event rate for the muon events is

$$\Gamma_{\mu} \simeq 3 \times 10^{-8} [a/(4 \times 10^6 \text{ cm}^2)] \text{ Hz}, \quad (3.9)$$

or about 1 event per year. Recall that the normalization A could easily be larger by a factor of 10 due to uncertainties in the photon flux, the photon duty cycle, or photon absorption.

Of course, this signal must be compared to the background of throughgoing cosmic-ray muons.²² This background depends strongly upon the zenith angle because the energy needed by a muon to penetrate to the detector depends upon the zenith angle, and the integrated flux of muons at the earth's surface decreases rapidly with muon energy. Taking the integrated muon flux at the surface of the earth to vary as

$$N_{\mu}(>E) \simeq 10^{-7} E^{-2} \text{ cm}^{-2} \text{ sr}^{-1} \text{ sec}^{-1}, \quad (3.10)$$

the rate at which background atmospheric muons pass through the detector at zenith angle γ is

$$d\Gamma_B/d\Omega \simeq a \times 10^{-7} E^{-2}(x) \text{ cm}^{-2} \text{ sr}^{-2} \text{ sec}^{-1} \simeq a \times 3 \times 10^{-11} E^{-2}(x) \text{ cm}^{-2} \text{ deg}^{-2} \text{ sec}^{-1} \simeq (a \times 10^{-10} \text{ Hz deg}^{-2}) [\exp(x_3) - 1]^{-2}, \quad (3.11)$$

where $E(x)$ is the energy (in TeV) a muon must have to reach the detector from the surface of the Earth:

$$E(x) \simeq \frac{1}{2} [\exp(x_3) - 1],$$

$$x(\gamma) \simeq R \left\{ -(1-d/R) \cos \gamma + [(1-d/R)^2 \cos^2 \gamma + 2d/R - (d/R)^2]^{1/2} \right\}$$

$$\simeq \begin{cases} d/\cos \gamma & [\text{for } \cos \gamma \geq (d/R)^{1/2}], \\ -2R \cos \gamma & [\text{for } \cos \gamma \leq -(d/R)^{1/2}], \end{cases}$$

$x = x_3$ 3 km, and $R \simeq 6500$ km is the radius of the earth. For IMB ($d \simeq 1.5$ km and $a \simeq 4 \times 10^6$ cm²) the background rate is approximately

$$d\Gamma_B/d\Omega \simeq (5 \times 10^{-4} \text{ Hz deg}^{-2}) [\exp(0.5/\cos \gamma) - 1]^{-2}. \quad (3.12)$$

The background muon rate decreases rapidly with increasing zenith angle, as is shown in Fig. 5. To obtain the background rate with which the signal from Cygnus X-3 must compete, one must multiply this rate per solid angle by the solid angle acceptance of the detector. For a cone with acceptance angle α

$$\Delta\Omega \simeq (2.1 \times 10^4 \text{ deg}^2) [1 - \cos(\alpha/2)].$$

The zenith angle of Cygnus X-3 varies between $\theta - \delta$

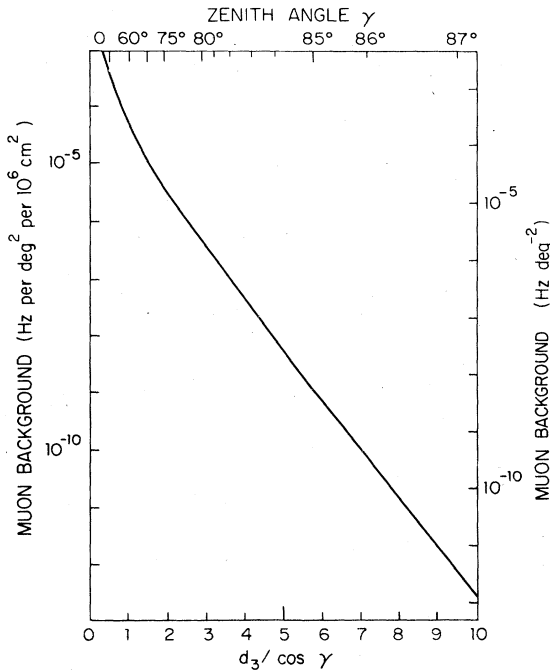


FIG. 5. The approximate background atmospheric muon rate [see Eq. (3.11)] as a function of $d_3/\cos \gamma \simeq x_3 \simeq x/3$ km. The scales on the top and right-hand side are those appropriate for a detector at a depth $d = 1500$ mwe with a cross section of 4×10^6 cm².

and $180^\circ - (\theta + \delta)$ with the sidereal period, where $\delta \simeq 40.8^\circ$ is the declination of Cygnus and θ is the latitude of the detector. For IMB θ is 41.5° N so that Cygnus X-3 only gets about 8° below the horizon.²³ As far as background goes, the deeper, more southern detectors such as the Kolar Gold Field ($\theta \simeq 12^\circ$ N) and the Case-Wit-Irvine mine ($\theta \simeq 26.5^\circ$ S) are much better off.

For completeness, consider the possibility that the neutrino spectrum is steeper than E^{-3} , in which case both the “contained” and “muon” events are dominated by the low-energy neutrinos:

$$\Gamma_\mu \simeq aA \times 3 \times 10^{-9} (E_{\min}/1 \text{ GeV})^{-n+3} 10^{3(n-2)}/(n-3), \quad (3.13)$$

$$\Gamma_c \simeq aA l_{10} 4 \times 10^{-9} (E_{\min}/1 \text{ GeV})^{-n+2} 10^{3(n-2)}/(n-2). \quad (3.14)$$

In this case the two rates are comparable, and the signal is unlikely to be detectable unless the flux of GeV neutrinos is many orders of magnitude greater than that of the photons, which in turn would imply an energy output in neutrinos much greater than 10^{38} erg sec⁻¹. We should emphasize this point; since the probability for a neutrino to produce a “muon” event varies either as E^2 (for $E < \text{few TeV}$) or as $E \ln(E)$ (for $E > \text{few TeV}$) and the neutrino luminosity only varies linearly with neutrino energy, the power required to produce a given event rate in the detector decreases with neutrino energy.

Finally, consider the Hillas model²⁴ where the observed photon flux is due to the electromagnetic shower produced by a monoenergetic beam of 10^5 TeV protons with luminosity of $\simeq 10^{39}$ erg sec⁻¹ which hits the companion star. In this model we would expect an approximately monoenergetic flux of neutrinos of energy a few $\times 10^4$ TeV, assuming that E_c is greater than 10^4 TeV. Assuming that about 10% of the beam energy goes into neutrinos of average energy $\langle E_\nu \rangle \simeq 10^4$ TeV, the resulting neutrino flux is

$$N_\nu \simeq \left(\frac{1}{10}\right) (10^{39} \text{ erg sec}^{-1}) \langle E_\nu \rangle^{-1} (4\pi r^2)^{-1} \simeq 10^{-12} \text{ cm}^{-2} \text{ sec}^{-1}. \quad (3.15)$$

Such a flux produces a muon event rate of

$$\Gamma_\mu \simeq (10^{-8} \text{ Hz}) [a/(4 \times 10^6 \text{ cm}^2)]. \quad (3.16)$$

More likely is the case that $E_c \leq 10^4$ TeV, so that the flux of 10^4 TeV neutrinos is due to “prompt” charm and heavy-flavor decays and is a factor of 100–1000 smaller than the above estimate, resulting in an event rate which is 10^{-2} – 10^{-3} of the above estimate. However, due to the fact that some reasonable fraction of the π 's and K 's that are produced will interact and lose energy until $E \lesssim E_c$ and they can decay in flight; a significant fraction, $f \simeq 10^{-1}$ – 10^{-2} , of the 10^{39} erg sec⁻¹ should come out in neutrinos of energy of the order of E_c (the pileup effect we discussed in the preceding section). In this case

$$N_\nu \simeq f \times (10^{39} \text{ erg sec}^{-1}) \times (E_c)^{-1} (4\pi r^2)^{-1} \simeq 10^{-9} (f/10^{-1}) (E_c/10 \text{ TeV})^{-1} \text{ cm}^{-2} \text{ sec}^{-1}. \quad (3.17)$$

This leads to a “muon” event rate of

$$\begin{aligned}\Gamma_\mu &\simeq aN_\nu P_\mu(E_c) \\ &\simeq (10^{-7} \text{ Hz})[a/(4 \times 10^6 \text{ cm}^2)](f/10^{-1}) \\ &\quad \times \ln[1 + E_c/(10 \text{ TeV})].\end{aligned}\quad (3.18)$$

Note that for $E_c \gtrsim$ few TeV the predicted event rate is only logarithmically dependent upon E_c . The predicted rate is slightly higher than in the case that $E_c \geq 10^4$ TeV because the cross section for $\nu_\mu + N \rightarrow \mu + X$ is still rising linearly with energy at 10 TeV, whereas at energies $\gtrsim 100$ TeV it rises only logarithmically.

IV. SUMMARY

To summarize, based upon two simple models^{2,24} where the high-energy γ rays from Cygnus X-3 are produced by a beam of energetic protons interacting with the envelope of the companion star, we have calculated the expected neutrino flux, normalized to the photon flux. Up to an energy where the pions and kaons, whose decays produce the bulk of the neutrinos, interact before they have time to decay, the neutrino flux is comparable to the photon flux. At higher energies the neutrino flux is primarily due to charm and heavy-flavor decays and the flux is down from that of the photons by a factor of about 100–1000. The source neutrino flux is modulated by absorption of neutrinos by the companion star, resulting in the energy-dependent neutrino light curves shown in Fig. 3. Normalizing the predicted neutrino flux to the observed γ ray flux results in a predicted muon event rate which might be detectable in a large, underground detector such as IMB. The predicted contained event rate is about 1000 times smaller. Most of the muon events are due to neutrinos of energy of 3–100 TeV and so should be heavy track. The predicted event rate could be significantly larger if the photon duty cycle is less than 5% or if there is significant absorption of UHE γ rays within the system.

If the spectrum of neutrinos is not $\propto E^{-2.1}$ as the present UHE- γ -ray data suggests, and is steeper than E^{-3} , then the number of contained and muon events will be comparable and dominated by GeV neutrinos. However, unless the flux of GeV neutrinos is many orders of magnitude greater than that of photons, the neutrinos will not be detectable in larger proton-decay detectors.

Finally, we should mention that if other very robust binary x-ray sources such as Vela X-1, LMC (Large Magellanic Cloud) X-4, and Her X-1 are also potent sources of UHE γ rays,²⁵ then they should produce high-energy neutrinos in a similar fashion. In particular, recent observations of the UHE γ -ray spectrum of Vela X-1 (Ref. 26) and TeV γ rays from Her X-1 (Ref. 27) indicate fluxes which are comparable to that of Cygnus X-3, suggesting that Vela X-1 and Her X-1 should produce comparable fluxes of high-energy neutrinos. If it is possible to detect neutrinos from systems like Cygnus X-3, the neutrino light curve can be used to infer the core density of the companion and E_c can be used to determine the density of the stellar envelope. Probing a system with a many-TeV neutrino beam of luminosity 10^{38} erg sec⁻¹ offers a multitude of new possibilities.

Note added. After this work was completed we learned of similar work by T. K. Gaisser and T. Stanev, Phys. Rev. Lett. **54**, 2265 (1985); V. S. Berezinsky, C. Castagnoli, and P. Galeotti, Instituto de Fisica Generale dell'Universita di Torino report, 1985; G. Cocconi, CERN report, 1985. These groups reached similar conclusions to ours.

ACKNOWLEDGMENTS

We wish to thank Chris Hill, J. D. Bjorken, David Seckel, David Schramm, John Learned, and Jim Stone for useful conversations. This work was supported by NASA (at Fermilab), the Department of Energy (at Fermilab, Chicago, and Indiana University), and by M.S.T.'s A. P. Sloan Fellowship.

¹D. R. Parsignault, J. Grindlay, H. Gursky, and W. Turker, *Astrophys. J.* **218**, 232 (1977).

²W. T. Vestrand and D. Eichler, *Astrophys. J.* **261**, 251 (1982).

³M. Milgrom, *Astron. Astrophys.* **51**, 215 (1976).

⁴P. Hertz, P. Joss, and S. Rappaport, *Astrophys. J.* **224**, 614 (1978).

⁵R. C. Lamb, C. E. Fichtel, R. C. Hartman, D. A. Kniffen, and D. J. Thomson, *Astrophys. J.* **212**, L63 (1977).

⁶Yu. I. Neshpor *et al.*, *Astrophys. Space Sci.* **61**, 349 (1979).

⁷S. Danahar, D.J. Fegan, N. A. Porter, and T. C. Weeks, *Nature (London)* **289**, 568 (1981).

⁸R. C. Lamb, C. P. Godfrey, W. A. Wheaton, and T. Turner, *Nature (London)* **296**, 543 (1982).

⁹M. Samorski and W. Stamm, *Astrophys. J.* **268**, L17 (1983); J. Lloyd-Evans, R. Coy, A. Lambert, J. Lapikens, M. Patel, R. Reid, and A. Watson, *Nature (London)* **305**, 784 (1983).

¹⁰J. M. Dickey, *Astrophys. J.* **283**, L71 (1983).

¹¹The observations suggest that the angle i between the normal

to the orbital plane and line of sight is about 90° and that the distance between the compact object and the companion star y is much less than R . If this is so, then θ , the angle between the point where the line of sight intersects the companion star and a line connecting that point to the center of the star, is equal to the phase angle ψ (see Fig. 1). The angle θ determines when the UHE- γ -ray pulses should occur ($\theta \simeq \pm \pi/2$) and the degree of neutrino absorption. For $i \neq 90^\circ$ and $y \neq 0$, θ and ψ are related by $\sin \theta = (1 + y/R)(\cos^2 i + \sin^2 i \sin^2 \psi)^{1/2}$, which has the limiting forms $\sin \theta = (1 + y/R)\sin \psi$, for $i = 90^\circ$, and $\cos \theta = \sin i \cos \psi$, for $y/R \ll 1$. Throughout this paper we have assumed that $i = 90^\circ$ and $y \ll R$.

¹²D. Eichler, *Nature (London)* **275**, 725 (1978).

¹³The astrophysical production of UHE γ and ν_μ 's from π decays and the possible detection of the ν_μ 's has been considered in more generality by, V. Stenger, *Astrophys. J.* **284**, 810 (1984), and references therein.

¹⁴See, also, F. W. Stecker, *Astrophys. J.* **228**, 919 (1979).

¹⁵Yu. M. Andreev, V. S. Berezinsky, and A. Yu. Smirnov, Phys. Lett. **84B**, 247 (1979).

¹⁶See, for example, D. Clayton, *Principles of Stellar Evolution and Nucleosynthesis* (McGraw-Hill, New York, 1968).

¹⁷In the text we have treated the interaction of the proton beam with the envelope of the star in a highly simplified way. A star being bombarded by 10^{38} – 10^{39} erg sec⁻¹ is not likely to resemble an ordinary star; however, for an ordinary star this problem can be treated much more precisely. In an ordinary star the amount of material above the photosphere (the shell in the star where the temperature equals the effective temperature of the star) is negligible, $\int_R^\infty \rho dl \simeq \text{few g cm}^{-2}$. Below the photosphere, in the envelope, $\rho \sim T^n$ ($n=3.25$ for a radiative envelope, appropriate for stars more massive than about $1.5M_\odot$; $n=1.5$ for a convective envelope, appropriate for stars less massive than about $1.5M_\odot$). The equations of hydrostatic equilibrium then imply a density run in the envelope: $\rho = \rho_0(d/h + 1)^n$, where d is the depth below the photosphere, h is the scale height $\simeq \text{few} \times 10^8$ cm, and ρ_0 is the density at the photosphere $\simeq 10^{-7}$ g cm⁻³. From this one can compute that $\int_0^d \rho dl \simeq \rho_0 h [(d/h + 1)^{n+1} - 1]/(n+1)$. It then follows that $\int_0^d \rho dl \simeq 100$ g cm⁻² at a depth $d \simeq 3h$. This means that π 's and K 's which are produced in the first 100 g cm⁻² have to traverse roughly a scale height ($\simeq 10^8$ cm) before they encounter another 100 g cm⁻². For a discussion of stellar envelopes, see, e.g., M. Schwarzschild, *The Structure and Evolution of the Stars* (Dover, New York, 1958).

¹⁸R. M. Bionta *et al.*, in *Science Underground*, proceedings of the Workshop, Los Alamos, 1982, edited by Michael Martin Nieto *et al.* (AIP, New York, 1983), p. 138.

¹⁹For convenience we have expressed all distances in their water equivalent values, i.e., $d_{we} = d(\rho/1 \text{ g cm}^{-3})$.

²⁰B. B. Rossi, *High Energy Particles* (Prentice-Hall, New York, 1952).

²¹For $\nu + N \rightarrow \mu^- + X$, $d\sigma/dy \simeq \text{constant}$, while for $\bar{\nu} + N$

$\rightarrow \mu^+ + X$, $d\sigma/dy \simeq \text{constant} \times (1-y)^2$; here $(1-y) = E_\mu/E_\nu$. This means that for $\nu + N \rightarrow \mu^- + X$, $\langle E_\mu \rangle \simeq E_\nu/2$, and for $\bar{\nu} + N \rightarrow \mu^+ + X$, $\langle E_\mu \rangle \simeq 3E_\nu/4$. The average range of a muon produced by a neutrino (or antineutrino) of energy E_ν is

$$\langle l \rangle = \int_0^{E_\nu} l(E_\mu) (d\sigma/dE_\mu) dE_\mu / \int (d\sigma/dE_\mu) dE_\mu .$$

For neutrino-produced muons: $\langle l \rangle \simeq l(cE_\nu)$, where depending upon E_ν , c varies between 0.5 and 0.37; for antineutrino-produced muons: $\langle l \rangle \simeq l(cE_\nu)$, where c varies between 0.72 and 0.75. For simplicity, in Eq. (3.4) we have taken $\langle l \rangle \simeq l(E_\nu/2)$.

²²There is an additional small background of throughgoing muons due to atmospherically produced neutrinos which interact in the rock surrounding the detector. Their flux is roughly isotropic. The rate for muons with energy greater than 2 GeV is $\simeq 8 \times 10^{-17}$ cm⁻² deg⁻² sec⁻¹, and with energy greater than 1 TeV is $\simeq 10^{-17}$ cm⁻² deg⁻² sec⁻¹. For further discussion, see T. K. Gaisser and T. Stanev, Phys. Rev. D **30**, 985 (1984).

²³The cosine of the zenith angle of Cygnus X-3 is given by $\cos \gamma = \sin \theta \sin \delta + \cos \theta \cos \delta \sin [2\pi t / (23h)(56m)]$, and so γ varies between $(\theta - \delta)$ and $[180^\circ - (\theta + \delta)]$. With the exception of the Kolar Gold Field detector, all existing large, underground detectors are between 36°N and 46°N latitude, so that Cygnus X-3 never gets much below the horizon at any of the detectors.

²⁴A. M. Hillas, Nature (London) **312**, 50 (1984).

²⁵G. Chanmugan and K. Brecher, Nature (London) **313**, 767 (1985).

²⁶R. J. Protheroe, R. W. Clay, and P. R. Gerhardy, Astrophys. J. **280**, L47 (1984).

²⁷J. C. Douthwaite, A. B. Harrison, I. W. Kirkman, H. J. Macrae, K. J. Orford, K. E. Turver, and M. Walmsley, Nature (London) **309**, 691 (1984).